

A case for a battery-aware model of drone energy consumption

Original

A case for a battery-aware model of drone energy consumption / Chen, Yukai; Baek, Donkyu; Bocca, Alberto; Macii, Alberto; Macii, Enrico; Poncino, Massimo. - ELETTRONICO. - (2018), pp. 1-8. (2018 IEEE International Telecommunications Energy Conference (INTELEC) Turin(Italy) 7-11 October 2018) [10.1109/INTLEC.2018.8612333].

Availability:

This version is available at: 11583/2723260 since: 2020-02-24T12:29:50Z

Publisher:

IEEE

Published

DOI:10.1109/INTLEC.2018.8612333

Terms of use:

This article is made available under terms and conditions as specified in the corresponding bibliographic description in the repository

Publisher copyright

(Article begins on next page)

A Case for a Battery-Aware Model of Drone Energy Consumption

Yukai Chen Donkyu Baek Alberto Bocca Alberto Macii Enrico Macii Massimo Poncino

*Department of Control and Computer Engineering
Politecnico di Torino
Torino, Italy*

{yukai.chen, donkyu.baek, alberto.bocca, alberto.macii, enrico.macii, massimo.poncino}@polito.it

Abstract—The market of small drones has been recently increasing due to their use in many fields of application. The most popular drones are multirotors, in particular quadcopters. They are usually supplied with batteries of limited capacity, and for this reason their total flight time is also limited.

As a consequence of the non linear characteristics of batteries, estimation of the real flight time may become an issue, since most battery models do not include all the non idealities. Consequently, applications such as delivery service, search and rescue, surveillance might not be accomplished correctly because of inaccurate energy estimations.

This paper describes a battery-aware model for an accurate analysis of the drone energy consumption; this model is then applied to a scenario of drone delivery. Results show an accuracy greater of about 16% with respect to the traditional estimation model.

Index Terms—Battery modeling; power/energy estimation; Unmanned Aerial Vehicles.

I. INTRODUCTION

In recent years, the utility of unmanned aerial vehicles (UAVs) or drones have increased in different application fields (e.g., monitoring, mapping, delivery) [1]. In this context, small drones are now very popular [2], such as multirotor helicopters also known as multicopters. As a consequence of the limited energy available from the small size lithium polymer (LiPo) batteries, which are typically installed on these mini drones, the energy consumption is a critical variable that impacts on various figures of merit (FOM). For instance, in a scenario of delivery services, the following should be considered:

- *quality of service* on meeting delivery deadlines;
- *throughput* regarding the number of packages delivered per charge cycle;
- *battery state-of-health* by reducing the number of charge cycles in a given time slot.

The key for assessing these quantities is a reliable power/energy consumption model, which allows a careful planning of a set of delivery tasks for a given drone configuration. In the literature, many such models have been proposed; they consider various parameters such as payload weight, flying altitude, UAV speed, and distance flown. These models combine the basic equations of flight dynamics and translate them into the electrical domain assuming the power is provided by an electrical motor [3], [4], [5]. The systematic

drawback of these models is that they are not battery-aware, i.e., they assume that the power drawn by the motor is in a 1:1 correspondence to the power drawn by the battery. This is not the case, however, since a battery supplies power with different efficiency values depending on its state-of-charge (SOC), and this efficiency is also non-linearly dependent on the amount of the power requested [6]. As a consequence, the omission of the real battery performance analysis may result in a wrong estimation of the real flight time of the drone [7].

In this work we will show how including battery awareness in a drone power model is essential to avoid significant mispredictions.

II. BACKGROUND AND RELATED WORK

A. Quadcopter Dynamics Fundamental Principles

Basically, there are three forces acting on a quadcopter as shown in Figure 1:

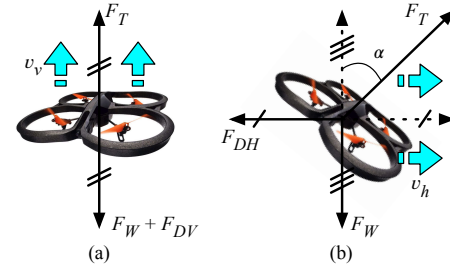


Figure 1. Forces acting on a drone.

F_W is the total weight of the drone with a payload, which pulls down the drone due to the force of gravity, whereas F_{DH} and F_{DV} are drag forces in horizontal and vertical direction, respectively, that are caused by the disruption of airflow. Drag opposes a movement of the drone in horizontal and vertical directions. F_T is the thrust produced by the rotating propellers of the drone; it opposes the weight and drag to sustain the height and speed of the drone. Figure 1(a) and Figure 1(b) show the overall forces when a drone moves vertically at a constant speed v_v , and flies horizontally at a constant speed v_h , respectively. The sum of the weight and drag equals to the thrust in both cases.

F_W , F_{DH} and F_{DV} are modeled by the following:

$$F_W = (m_d + m_p)g \quad (1)$$

$$F_{DV} = \frac{1}{2}\rho A_t C_d v_v^2; \quad F_{DH} = \frac{1}{2}\rho A_f C_d v_h^2 \quad (2)$$

where m_d and m_p are the mass of the drone and payload, respectively, g is the gravity acceleration, A_f and A_t are the cross sectional areas in horizontal and vertical directions, C_d is a drag coefficient, and ρ is the air density. The required thrusts $F_{T,v}$ and $F_{T,h}$ are then described as:

$$F_{T,v} = F_W + F_{DV} = (m_d + m_p)g + \frac{1}{2}\rho A_t C_d v_v^2 \quad (3)$$

$$F_{T,h} = \sqrt{F_W^2 + F_{DH}^2} = \sqrt{((m_d + m_p)g)^2 + \left(\frac{1}{2}\rho A_f C_d v_h^2\right)^2} \quad (4)$$

The thrust to oppose the weight and drag is obtained through the induced air passing a rotating propeller as shown in Figure 2. A basic formula for thrust is the following:

$$F_T = 2\rho A_p v_i^2 \quad (5)$$

where A_p is the disk area of the propellers, and v_i is the induced air flow velocity.

The power consumption necessary to induce thrust is derived simply as:

$$P_T = F_T v_i = \sqrt{\frac{T^3}{2\rho A_p}} \quad (6)$$

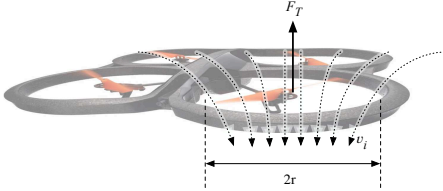


Figure 2. Thrust by rotating propeller.

However, the power consumed by the actual motors differs from the power obtained by dynamics because of the efficiencies of the motor angular speed and torque. In this context, it is possible to estimate an accurate power consumption by measuring the power with respect to the motor angular speed. The higher motor angular speed, the higher induced air passing the propellers, thus higher thrust.

F_T , in terms of motor angular speed, is then modeled by:

$$F_T = \frac{1}{2}N\rho A_p C_t (\omega r)^2 \quad (7)$$

where N is the number of rotors, C_t is a thrust coefficient, ω is the angular speed of the rotors, and r is the radius of the propellers. In general, C_t has a value in a range from 0.01 to 0.05 [8]. Therefore, for a given drone flight, We can easily

solve the required thrust for a given drone flight from (1)–(4) and the required angular speed to obtain the required thrust from (7). The maximum payload and maximum horizontal speed are bounded by the maximum angular speed of the motor speed.

B. Related Works

Nowadays, drones are used in so many different contexts such as emergency services in humanitarian operations (e.g., *search and rescue*), traffic surveillance, package delivery tasks, telemetry and mapping, among others [1], [9], [10].

In the literature, various algorithms have been proposed for energy-aware path planning for UAVs. However, most works do not consider a real performance analysis of the battery. For instance, in [11] the authors face the problem of the minimum-energy path through a model for brushless DC motors and solve it with respect to the angular acceleration of the propellers of a quadrotor. In [3], the authors present an algorithm that solves the problem of minimizing the total energy of the IRIS quadrotor, in the application of area coverage in photogrammetry, through a power model that characterizes the consumption of the drone operating in different conditions. However, also in this case the electrical energy source is not considered. On the other hand, in [12] the authors analyzed the performance of different LiPo batteries applied to AR Drone 2.0. In this case, the models considered for battery runtime are related to the capacity rate effect, even the Peukert's law [13]. Nevertheless, the experimental results show, as expected, a difference with respect to the data obtained from these models.

For small UAVs, both fixed wings and multirotors, an altitude controller based on battery SOC is described in [14]. In this case, the battery model relies on the equivalent electrical circuit of [6] applied to LiPo batteries, and the relationship between nominal thrust and battery SOC is also provided.

Routing optimization for drone delivery service was analyzed in [4]; however, the proposed power model only includes the weight of the battery, in addition to payload. In this context, a model for solving the problem of minimization of the delivery time for a certain number of packages, is provided in [15]. In this case, the battery performance is however considered just from a service time point of view.

III. PROPOSED BATTERY-AWARE MODEL

Firstly, from (1)–(7) we derive the motor angular speed necessary for a drone (i) to fly at a constant horizontal speed v_h and (ii) to move at a constant vertical speed v_v with a payload weight w_p (i.e., $w_p = m_p \cdot g$), during vertical take-off and landing (VTOL):

$$\omega_h = \frac{(4(m_d + m_p)^2 g^2 + \rho^2 A_f^2 C_d^2 v_h^4)^{1/4}}{(r^2 \rho A_p C_t)^{1/2}} = f_h(w_p, v_h) \quad (8)$$

$$\omega_v = \frac{(2(m_d + m_p)g + \rho A_t C_d v_v^2)^{1/2}}{(r^2 \rho A_p C_t)^{1/2}} = f_v(w_p, v_v) \quad (9)$$

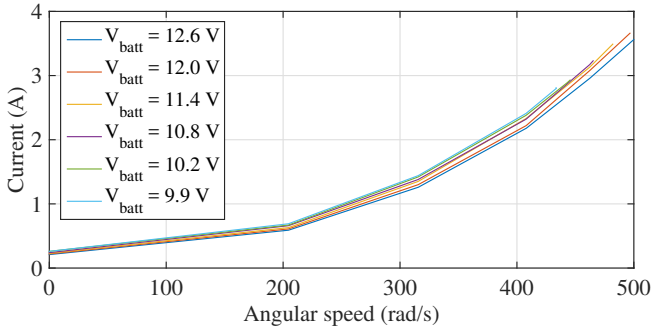


Figure 3. Drone battery current versus motor angular speed [16].

We refer to the experimental data of [16] about motor current, voltage and angular speed for quadcopter Parrot AR.Drone 2.0. They also include the related motor efficiency. Figure 3 reports the characteristics of the *motor current vs. angular speed* at different battery voltages. The function g for the motor power consumption P dependent on angular speed ω (max. 500 rad/s), is then extracted by fitting these experimental data to a polynomial as follows:

$$P \approx g(\omega) = 2.258 \cdot 10^{-07}\omega^3 + 3.866 \cdot 10^{-05}\omega^2 + 5.137 \cdot 10^{-3}\omega + 2.616. \quad (10)$$

Finally, the motor power consumptions P_h and P_v for horizontal and vertical flight, respectively, are obtained as functions of both payload and speed by plugging the expressions of ω_h and ω_v in (8) and (9), respectively, into (10):

$$P_h(w_p, v_h) \approx g(f_h(w_p, v_h)) \quad (11)$$

$$P_v(w_p, v_v) \approx g(f_v(w_p, v_v)) \quad (12)$$

A. Characterization of a Delivery Task

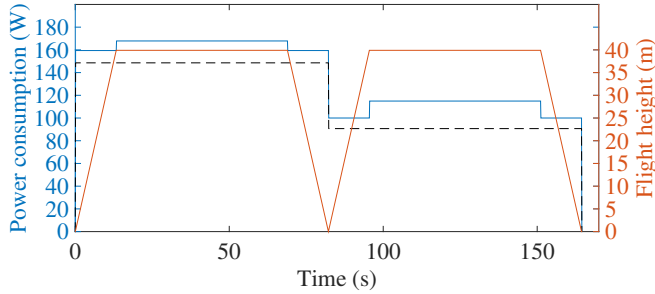


Figure 4. A drone flight model (a) going to place B with a payload and (b) returning to place A without payload.

The multi-plot chart in Figure 4 shows the power consumption of a drone during the task of delivering a parcel (weight w_p) from location A to location B:

- 1) in place A, take-off at constant vertical speed v_v until reaching a given height h ;
- 2) horizontal flight at constant speed v_h for the entire distance d ;
- 3) in place B, landing at the same vertical speed v_v .

- 4) Then, the drone returns to the place A without the payload.

In this scenario, the initial acceleration and final deceleration during VTOL and horizontal flight are neglected. The delivery distance d is 500 m, payload w_p is 300 g and the horizontal velocity v_h is 7 m/s. The gray horizontal dashed lines indicates hovering power ($v_h = v_v = 0$) with and without the payload. An important note: in general the maximum payload for AR.Drone 2.0 is about 200 g; however, in order to show how in general payload affects the energy consumption of a drone, we do not consider loss power for the effect of turbulence during take-off and landing, acceleration to approach v_v or v_h , and stability during the flight. Then, in this scenario the power model allows virtually a greater payload than the aforementioned value.

So, the overall energy consumption for one delivery is simplified by

$$E \approx P_v(w_p, v_v) \frac{h}{v_v} + P_h(w_p, v_h) \frac{d}{v_h} + P_v(w_p, -v_v) \frac{h}{|-v_v|} + P_v(0, v_v) \frac{h}{v_v} + P_h(0, v_h) \frac{d}{v_h} + P_v(0, -v_v) \frac{h}{|-v_v|}. \quad (13)$$

We assume the vertical speed v_v of 3 m/s, which is the maximum vertical speed of AR.Drone 2.0, whereas, the height h is 40 m.

Figure 5 shows the relationship of P_h by horizontal flight speed v_h and payload w_p . The power consumption at $v_h = 0$ coincides with the hovering power, whereas it is almost constant when the drone flights slower than 4 m/s; in truth, it increases at faster speeds because the drag forces are no longer negligible.

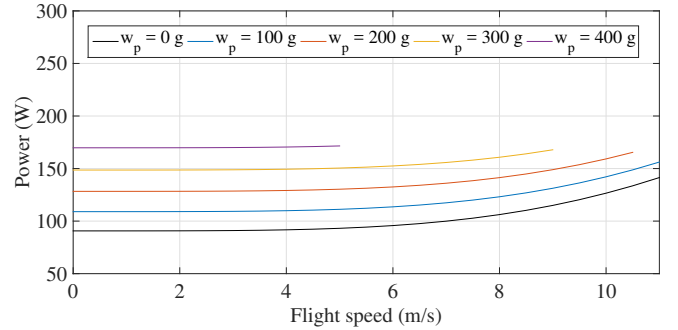


Figure 5. Drone motor power vs. flight speed and payload.

In (13), the energy for a given delivery task is mostly a 3-variable function of weight w_p , distance d , and horizontal flight speed v_h . In general, the maximum horizontal speed decreases with payload because the maximum thrust opposing the weight and drag is bounded by the maximum motor angular speed. Moreover, there is an energy-optimal horizontal speed for a given delivery task. A drone flying at too slow horizontal speed, causes a huge energy consumption because it consumes most energy to maintain the altitude during the long delivery time. On the other hands, too fast horizontal speed

increases air drag, which is proportional to the square of the horizontal speed. Therefore, the energy-optimal speed should be increased as the payload increases, in order to reduce the delivery time. Section IV provides various 3D plots for these characteristics, as a result for the scenario considered in this work.

B. Battery-Aware Energy Model

The battery current at different voltage (see Figure 3) and the drone power model refer to *the drone hardware*. Next step is to map their relation to relevant quantities such as weight, distance, and delivery time as a consequence of the flight speed, in order to estimate the real energy consumption of the drone. This step requires facing the following issues: *load current-dependent battery efficiency* and *non-ideal conversion efficiency*.

1) *Current-dependent battery efficiency*: In general, product data reports the nominal capacity of a battery as the total energy capacity after considering the constant discharge current depleting the battery in one hour. Nonetheless, higher the current, smaller is the total available energy of the battery during runtime. This effect is called *rated capacity*. It is present in both primary (non-rechargeable) and secondary (rechargeable) battery cells. In the case of primary cells, this effect is normally visible in *voltage vs. time* multi-plot charts. For secondary cells, it is typically expressed in *voltage vs. discharge capacity* multi-plot charts.

In addition, as a consequence of the rated capacity effect, there is another side effect: as the battery SOC decreases, for instance at constant power, the discharge current increases as well as the battery voltage decreases; therefore, the battery typically depletes faster than expected. As a consequence of these effects, mapping the drone energy to battery energy requires a conversion adapted to the real characteristics of the energy source, instead of considering a direct conversion. For these reason, we adopt a *battery model* that is able to analyze the energy necessary for accomplishing a certain task (after considering the flight speed, payload and distance) with respect to the real battery SOC. For this purpose, we use the model by [17], in which the well-known equivalent electrical circuit model of [6] is extended in such a way that it can track the SOC depletion based on the dynamics of the load current.

In the scenario of drone delivery service, the related battery power model is defined through an offline pre-characterization, as described in Section III-B3.

2) *Conversion Efficiency*: Most battery-powered devices require an electronic block for leveling the battery voltage to the load. In the context of small multirotors, this block is typically a DC/DC converter. In the case of a switching converter, the conversion efficiency is also non-linear, and it depends mainly on the voltage difference between input and output and the load current [18]. In general, the best efficiency is obtained at medium current load, while very low/high currents typically lead to a worst conversion efficiency. In this paper, we assume this efficiency to be constant in order to focus on the first effect.

3) *Construction of the Power Model*: The flow chart in Figure 6 describes the main steps for generating the battery-aware power model, which consists of a 5-dimensional table (i.e., \mathbf{T}).

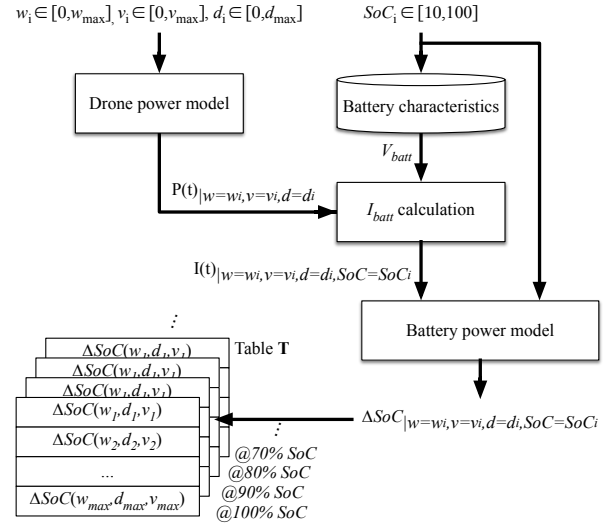


Figure 6. Offline Model Characterization.

The five parameters are the following: payload w , distance d , flight speed v , initial SOC in percentage (these are the input data), and the decrease of SOC (i.e., Δ SOC) as a result. Table \mathbf{T} stores all the possible Δ SOC for a given task of delivery service after considering the initial battery SOC.

In order to translate the drone power profile $P(t)$ into the battery-aware power model, and starting from the battery characteristics, we extract the battery current $I_{batt}(t)$ after considering the voltage V_{batt} at the beginning of the service. Then, we apply this current profile to the battery model. Finally, the amount of Δ SOC is stored into table \mathbf{T} .

From a computational cost of view, the complexity of the model and the size of \mathbf{T} is determined by the number of discretized levels of the parameters:

- $|W| = 4$ for payload $w \in [100, 400]$, step=100 g
- $|D| = 10$ for distance $d \in [100, 1000]$, step=100 m
- $|V| = 10$ for speed $s \in [1, 10]$, step=1 m/s
- $|S| = 10$ for initial $SOC \in [10, 100]$, step=10%.

The characterization process of the power model is fully implemented in an automatic way through a Python program.

4) *Usage of the Power Model*: After generating table \mathbf{T} , the pre-feasibility analysis of a sequence of delivery tasks requires to select the optimal battery-aware flight speed based on the initial SOC when starting the task. Figure 7 shows a diagram of these steps. In the example, for task τ_a with payload w_a , delivery distance d_a , and initial battery SOC SoC_a , we extract from the projection $\mathbf{T}(v)|_{w=w_a, d=d_a, SOC=SoC_a}$ of \mathbf{T} the optimal flight speed $v_{opt,a}$ at the minimum ΔSoC , which is ΔSoC_a . At the end, the current battery SOC is updated as $SoC_a - \Delta SoC_a$. This process is then repeated for all the next tasks.

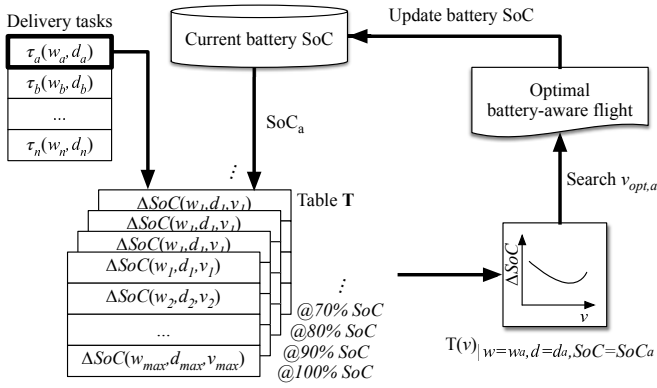


Figure 7. The optimal battery-aware flight using table T.

IV. RESULTS

A. Simulation Experiment Setup

For our simulations we selected the quadcopter AR Drone 2.0 Elite Edition made by Parrot manufacturer, because of the comprehensive measurements data provided in [16]. That document describes two measurement experiments: one concerns the angular speed of the rotors, torque, thrust and motor current at constant supply voltage, whereas the other concerns the same measurements but at varying voltages, as shown in Figure 3. The latter allows us to build the drone power consumption model as described in Section III.

In terms of energy source device, we used the Ultimate PX-04 LIPO battery, whose single cell physical parameters are shown in Table I. We considered a battery pack composed by four cells connected in series, in order to increase the total capacity to 4,000 mAh; in addition, we assumed the four battery cells to be ideally balanced. Then, we followed the methodology proposed in [17] to populate the circuit-equivalent battery model, which is characterized to the different discharge current rates provided by the battery datasheet.

Table I
MANUFACTURER'S PARAMETERS OF THE SELECTED BATTERY.

Parameters	Ultimate PX-04 LIPO
Dimension	104x8.75x6.25 mm
Rated Capacity	1000 mAh
Nominal Voltage	11.1 V
Cut-off voltage	9.0 V

As mentioned in the Section III-B2, we assumed the converter efficiency between drone motor and battery to be constant, and set at 90%. The whole system under our simulation is composed of one circuit equivalent battery model and the drone motor power consumption mathematical equation model. We implemented it by using SystemC as it supports multiple MoCs (Model of Computation) for modeling the drone motor and battery using different ways, whereas the extension version SystemC-AMS provides Electrical Linear Network (ELN) MoC, which facilitates constructing circuit equivalent models.

B. Deriving Battery-Aware Power Model of the Drone

We followed the characterization of our proposed battery-aware drone power model through the methodology described in Section III-B. We ran the simulation for different distances of delivery, payloads, and horizontal speeds. The specific values of these quantities are reported in Table II, where each set of data includes the minimal and maximum values of the interval for a specific parameter, and the step value. In addition, for each simulation we included the initial battery SOC at the beginning of each task, as defined in Section III-B.

As indicated in [19] the maximum weight of payload carried by the drone is 200 g, while to make our exploration space wider, we set the maximum weight of payload at 400 g. This is not in conflict with the realistic situation since we do not consider some power losses, as described in Section III-B3, and because our simulation results even demonstrate that the delivery tasks with 400 g cannot be delivered for long distances and low speeds.

Table II
SPECIFIC VALUES OF DISTANCE, PAYLOAD, SPEED FOR DERIVING PROPOSED BATTERY-AWARE POWER MODEL.

Variable Parameters	Set of values
Distance (m)	100:100:1000
Speed (m/s)	1:1:10
Payload (g)	100:100:400

In the following sub-sections, we firstly show the drone power consumption dependence on the distance of delivery, weight of payload and its speed; secondly, we show the drone energy consumption under different levels of battery SOC at the beginning of the delivery task, which is the main contribution in this work.

1) *Energy consumption dependence on Distance, Payload and Speed:* Due to space limitation, only a subset of the results about the weight of dependence of the battery energy on the parameters, is reported. The subplots in the first row of Figure 8 show ΔSOC , that is the energy consumption for each task under 100% initial SOC and different distances of delivery. The results show that ΔSOC increases with increasing distance. It is worth notice that ΔSOC equals to zero under the case of 800 m distance, 0.4 kg payload and 1 m/s speed, as shown in the fourth subplot of the first row in Figure 8; it means that the battery cannot provide enough energy for such delivery task.

Figure 9 illustrates similar results about the dependence on horizontal speed and distance of delivery: ΔSOC has a positive proportional relation to the weight of payload. However, the ΔSOC dependence on horizontal speed has an inversely-proportional relationship, as indicated in Figure 10. In general, the drone consumes less energy when it travels at high horizontal speed during the task; therefore, low speed is not really optimal for the drone from the point of view of energy. The reason is that the hovering power is a constant value during the flying time, and it requires a relatively high horizontal speed to be compensated.

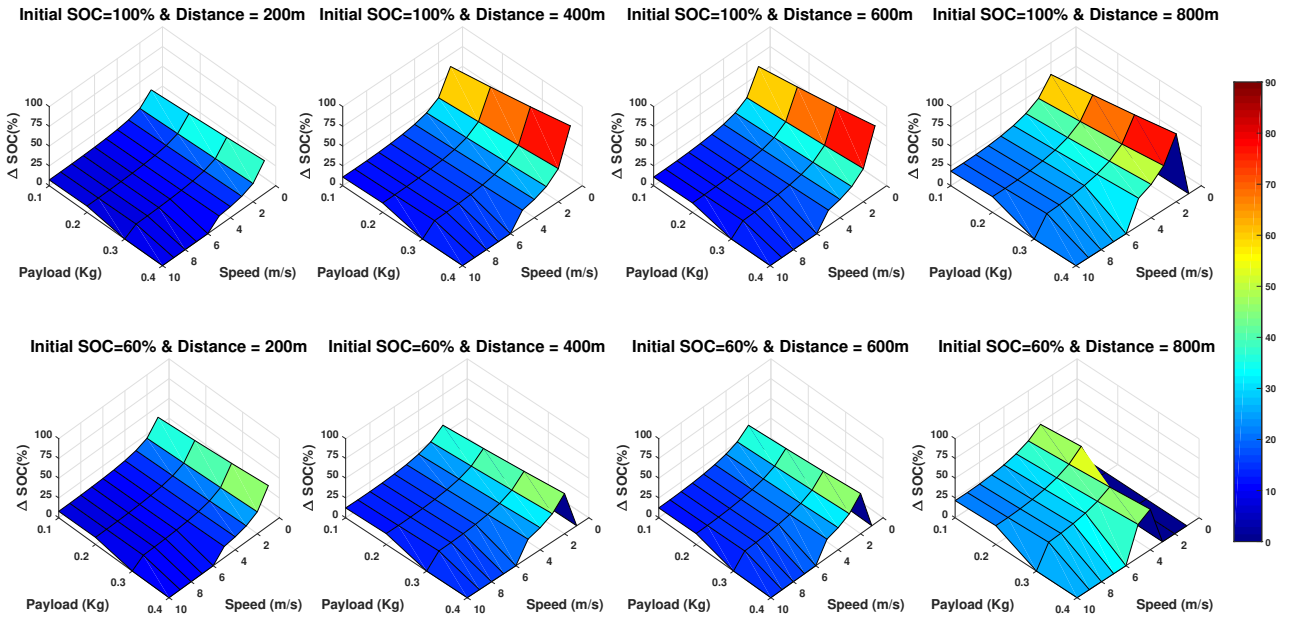


Figure 8. Energy consumption under fixed initial SOC of battery and delivery distance situations with two different initial SOC.

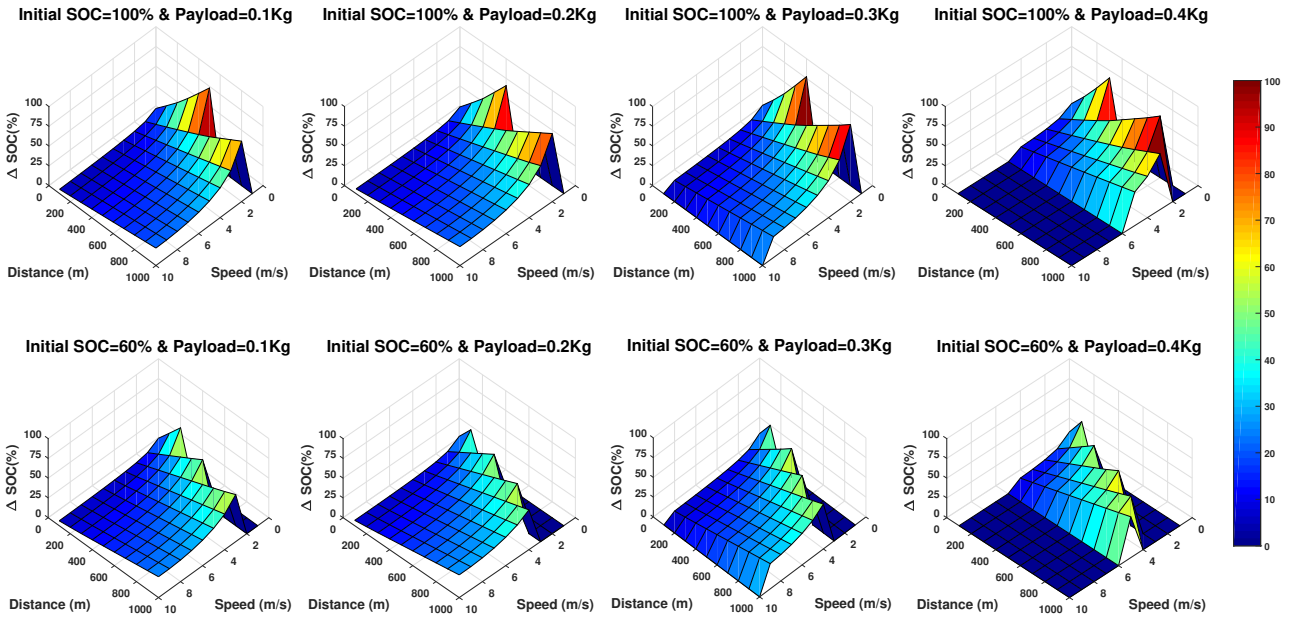


Figure 9. Energy consumption under fixed initial SOC of battery and delivery payload situations with two different initial SOC.

2) *Energy consumption dependence on SOC of battery:*
 Our main contribution of this work is deriving a battery-aware power model of drone by investigating the dependence of the power consumption on the battery SOC. In order to indicate how the proposed model accounts for the dependence of the drone energy consumption on the battery characteristics,

we conducted various simulations to calculate the energy consumption at different distance, speed, payload and initial battery SOC from 10% to 100% with 10% step. Due to space limitation, we only show two cases with different battery SOC at the beginning of the delivery task. However, the results from all the cases demonstrate that the drone consumes more and

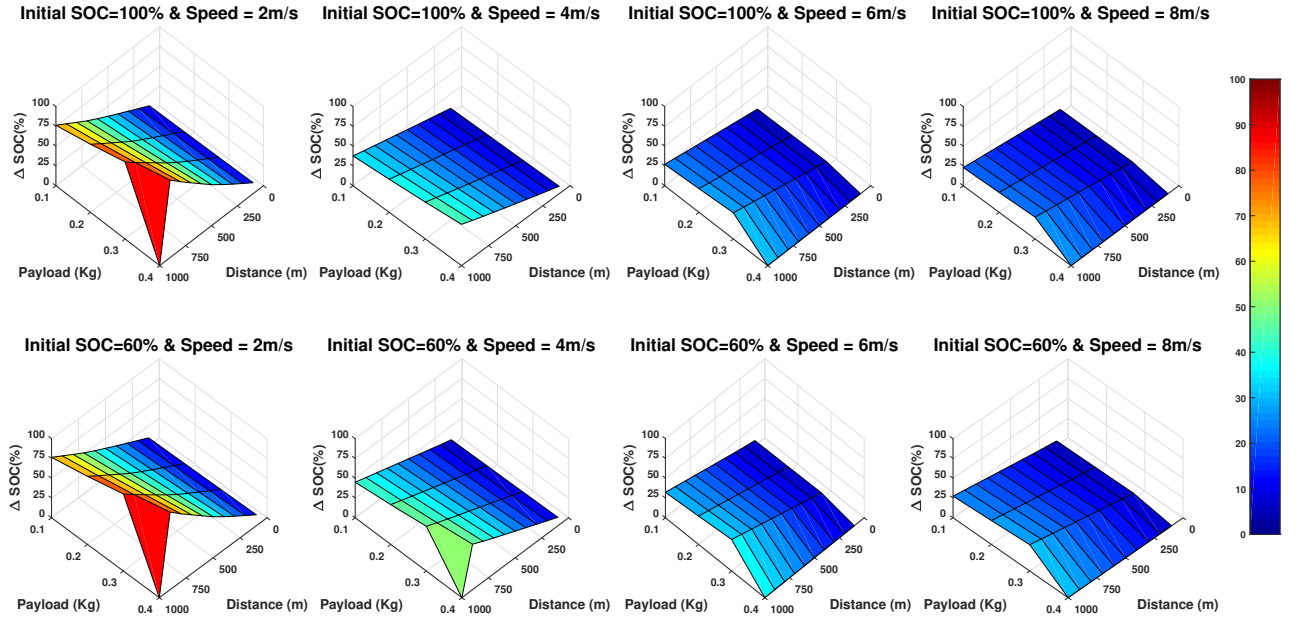


Figure 10. Energy consumption under fixed initial SOC of battery and horizontal speed situations with two different initial SOC.

more energy while the SOC of the battery decreases.

The ΔSOC values in the first row of Figures 8, 9 and 10 represent the energy consumption when the battery SOC is 100% at the beginning of the delivery, while the ΔSOC values of initial SOC of battery is 60% as shown in the second row of each figure. There are apparently differences between the subplots in the first and second rows of each figure, when analyzing some specific situations such as the long distance of delivery shown in Figures 8, heavy weight of payload indicated in Figures 9, and low horizontal speed revealed in Figures 9. Obviously, the number of undeliverable tasks increases under 60% initial SOC cases, especially in the case of long distance, heavy weight of payload and low horizontal speed, as shown in Figure 9. In fact, in this context 0 of ΔSOC represents that the battery does not have enough energy to accomplish the delivery task. This results means that the proposed model plays a decision-making role to determine the specific tasks that can be executed.

C. A case study of the proposed battery-aware model used as an accurate SOC estimator

For the purpose of illustrating how the proposed model can be beneficial in a general delivery task scheduling framework, we present a case study in order to demonstrate how this model improves the estimation accuracy with respect to a traditional model ignoring the battery non-idealities. In this scenario, a drone for deliveries has to carried out a number n of tasks $\{\tau_1, \dots, \tau_n\}$. Each task $\tau_i = (w_i, d_i)$ is characterized by a payload having weight w_i , and a target distance d_i . We assume that the drone delivers packages, one task at a time, until its battery is mostly fully depleted. In addition, time constraints

or other priorities for delivery are not here considered as our objective is to minimize the energy required to carry out the n deliveries, and the case study is generated just for the purpose of demonstrating the usefulness of the proposed energy model.

According to the statement of [20], the best scheduling policy of multiple delivery tasks always starts with the task having the heaviest payload and longest distance, because the battery is more efficient in providing larger currents when fully charged; therefore, an effective scheduling policy would be *heaviest-and-longest-first*. Consequently, the optimal scheduling policy can be determined in advance.

In order to analyze the real number of tasks can be really accomplished, we adopted this scheduling policy on the task set listed in Table III, and then we compared the results of the proposed energy model against the classical one.

Table III
DELIVERY TASKS WITH VARIOUS PAYLOADS AND DISTANCES.

Task	Weight (g)	Distance (m)	No. of Items
A	100	200	2
B	300	200	2
C	400	500	1
D	400	700	1

The optimal scheduling is then $D \rightarrow C \rightarrow B \rightarrow B \rightarrow A \rightarrow A$. The comparison of the battery SOC during simulation, after considering the proposed battery-aware model and the traditional one, is shown in Figure 11. The upper subplot indicates the battery is depleted during the last delivery task, according to the proposed model, as the total runtime of the battery is indeed 992 s. On the contrary, when considering the traditional model the residual battery SOC is overestimated to

15.98% after delivering all the tasks, as the bottom subplot shows.

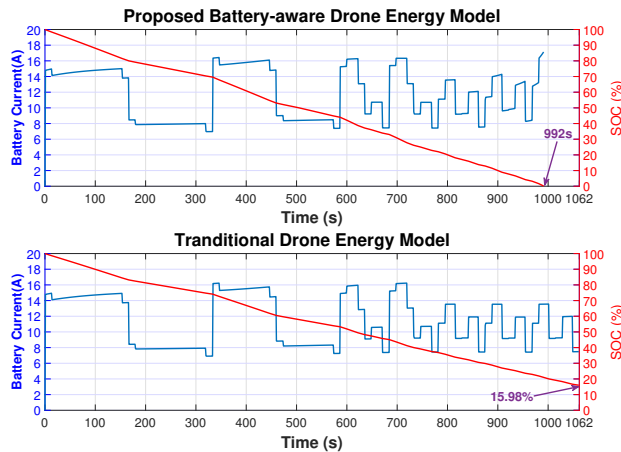


Figure 11. Battery current and SOC profiles of proposed battery-aware model and traditional model.

Therefore, when evaluating the two models, the difference in the estimation of the battery SOC is about 18%. The reason of this result is that the traditional model ignores the non-ideal characteristics of the battery during the discharge phase. In this scenario, the drone will land unexpectedly before ending all the tasks. On the other hand, our proposed model can be useful to avoid starting and executing delivery tasks that could not be accomplished if the real energy level of the battery is actually insufficient.

V. CONCLUSION

The remarkable rise of small drones with their many applications, requires a very detailed model for both mechanical and electrical parts, in order to predict correctly the true performance of these UAVs, which have generally very limited energy. This paper demonstrates that a model accounting for the non-linear characteristics of the battery, is essential from this point of view to estimating the real state-of-charge of the battery. A case study for a quadrotor operating at different working conditions was analyzed. In particular, simulations of various delivery tasks at different distance, payload, and horizontal speed were conducted. Results showed that a failure to take into account the real battery performance, leads to a notable inaccuracy about the estimation of the available energy and, consequently, of the overall flight time.

REFERENCES

- [1] S. Chen, D. F. Laefer, and E. Mangina, "State of technology review of civilian UAVs," *Recent Patents on Engineering*, vol. 10, no. 3, pp. 160–174, 2016.
- [2] D. Floreano and R. J. Wood, "Science, technology and the future of small autonomous drones," *Nature*, vol. 521, no. 7553, p. 460, 2015.
- [3] C. Di Franco and G. Buttazzo, "Energy-aware coverage path planning of UAVs," in *2015 IEEE International Conference on Autonomous Robot Systems and Competitions (ICARSC)*, 2015, pp. 111–117.
- [4] K. Dorling, J. Heinrichs, G. G. Messier, and S. Magierowski, "Vehicle routing problems for drone delivery," *IEEE Transactions on Systems, Man, and Cybernetics: Systems*, vol. 47, no. 1, pp. 70–85, January 2017.
- [5] K. Goss, R. Musmeci, and S. Silvestri, "Realistic Models for Characterizing the Performance of Unmanned Aerial Vehicles," in *Proc. 26th International Conference on Computer Communication and Networks (ICCCN)*, 2017, pp. 1–9.
- [6] M. Chen and G. Rincón-Mora, "Accurate electrical battery model capable of predicting runtime and IV performance," *IEEE Transactions on Energy Conversion*, vol. 21, no. 2, pp. 504–511, 2006.
- [7] D. Aleksandrov and I. Penkov, "Energy consumption of mini UAV helicopters with different number of rotors," in *11th International Symposium Topical Problems in the Field of Electrical and Power Engineering*, 2012, pp. 259–262.
- [8] S. Newman, *The foundations of helicopter flight*. Halsted Press, 1994. [Online]. Available: <https://books.google.it/books?id=3LhTAAAMAAJ>
- [9] I. Gkotsis, G. Eftychidis, and P. Kolios, "The use of UAS in disaster response operations," in *Fifth International Conference on Remote Sensing and Geoinformation of the Environment (RSCy2017)*, vol. 10444. International Society for Optics and Photonics, 2017, p. 104440W.
- [10] J. Scott and C. Scott, "Drone delivery models for healthcare," in *Proceedings of the 50th Hawaii International Conference on System Sciences (HICSS)*, 2017, pp. 3297–3304.
- [11] F. Morbidi, R. Cano, and D. Lara, "Minimum-Energy Path Generation for a Quadrotor UAV," in *2016 IEEE International Conference on Robotics and Automation (ICRA)*, 2016, pp. 1492–1498.
- [12] A. Abdilla, A. Richards, and S. Burrow, "Power and endurance modelling of battery-powered rotorcraft," in *2015 IEEE/RSJ International Conference on Intelligent Robots and Systems*, September 2015, pp. 675–680.
- [13] N. Omar, P. Van den Bossche, T. Coosemans, and J. Van Mierlo, "Peukert revisited — Critical appraisal and need for modification for lithium-ion batteries," *Energies*, vol. 6, no. 11, pp. 5625–5641, 2013.
- [14] M. Podhradský, C. Coopmans, and A. Jensen, "Battery state-of-charge based altitude controller for small, low cost multirotor unmanned aerial vehicles," *Journal of Intelligent & Robotic Systems*, vol. 74, no. 1-2, pp. 193–207, 2014.
- [15] S. Poikonen, X. Wang, and B. Golden, "The vehicle routing problem with drones: Extended models and connections," *Networks*, vol. 70, no. 1, pp. 34–43, 2017.
- [16] N. L. M. Jeurgens, "Implementing a Simulink controller in an AR.Drone 2.0," DC 2016.005, Eindhoven University of Technology, January 2016.
- [17] Y. Chen, E. Macii, and M. Poncino, "A circuit-equivalent battery model accounting for the dependency on load frequency," in *Proceedings of the Conference on Design, Automation & Test in Europe (DATE)*, 2017, pp. 1177–1182.
- [18] K. Chang, P. Rammos, S. A. Wilkerson, M. Bundy, and S. Andrew Gadsden, "LiPo battery energy studies for improved flight performance of unmanned aerial systems," in *Proceedings Volume 9837, Unmanned Systems Technology XVIII.*, 2016, p. 98370W.
- [19] Z. Liu, Z. Li, B. Liu, X. Fu, I. Raptis, and K. Ren, "Rise of mini-drones: Applications and issues," in *Proceedings of the 2015 Workshop on Privacy-Aware Mobile Computing*. ACM, 2015, pp. 7–12.
- [20] D. Baek, Y. Chen, A. Bocca, A. Macii, E. Macii, and M. Poncino, "Battery-aware energy model of drone delivery tasks," in *Proceedings of the International Symposium on Low Power Electronics and Design (ISLPED)*, 2018.